Visual Abstract

Elastic and nonlinear crack tip solutions comparison with respect to failure probability

Valery Shlyannikov, Andrey Tumanov, Natalia Boychenko
FRC Kazan Scientific Center of Russian Academy of Sciences, Russia
shlyannikov@mail.ru, http://orcid.org/0000-0003-2468-9300
tumanoff@rambler.ru, http://orcid.org/0000-0002-2345-6790
tasha1203@mail.ru

ABSTRACT. This study represents a methodology to assess the probability of failure based on three the driving force formulations defined by the corresponding brittle and ductile fracture criteria for compact and bending specimens made of 34XH3MA and S55C steels. The elastic stress intensity factor (SIF) and two types of the non-linear plastic SIFs were considered as the driving force or generalized parameter (GP) to determine the probability of failure assuming a three-parameter Weibull distribution. The elastic SIF were experimentally obtained for studied materials and specimen geometries whereas the plastic SIFs were numerically calculated for the same material properties, specimen configurations and loading conditions according to classical J_2 and strain gradient plasticity theories. Different specimen types with varying relative crack lengths and thicknesses were investigated. Proposed the normalized generalized parameter accounting for brittle or ductile fracture can be used as a suitable failure variable that is confirmed by comparison of the obtained failure cumulative distribution functions based on the three studied GPs.

KEYWORDS. Failure probability; Weibull distributions; Nonlinear stress intensity factors; Generalized parameters.

OPEN ACCESS

Citation: Shlyannikov, V., Tumanov, A., Boychenko, N., Elastic and nonlinear crack tip solutions comparison with respect to failure probability, Frattura ed Integrità Strutturale, 61 (2022) 1-13.

Received: 10.07.2022
Accepted: 19.07.2022
Online first: 20.07.2022
Published: 01.10.2022

INTRODUCTION

The main objective of experimental studies in fracture mechanics is to determine the critical value of a parameter characterizing the failure of a material. In most cases, the results of experimental studies must be evaluated statistically owing to the scatter of the critical fracture resistance parameter. If the fracture parameter is chosen correctly and the measuring instruments provide the required accuracy, the dispersion density corresponds to the normal Gaussian–Laplace distribution [1]. To evaluate the fracture resistance parameters and probability of failure, it is convenient

to use the Weibull distribution function [2]. The analysis of the Weibull parameters suggests that the studied characteristic is applicable as a fracture criterion.
The generalized probabilistic local approach (GPLA), developed by Muniz-Calvente et al. [3–7], allows the primary failure cumulative distribution function (PFCDF) owning to a certain failure type to be determined for a given material from experimental data and used subsequently for probabilistic design. Such approach introduce a realistic safety boundary provided that the failure criterion represented by an adequate generalized parameter (GP) and the corresponding failure criterion is properly recognized as a reference variable to be considered in the failure assessment.
The authors [3] supposed that the three-parameter Weibull distribution could be extended to any type of failure using the driving force ($\boldsymbol{X}_c$) defined by the corresponding fracture criterion. This methodology is feasible to apply for any kind of failure provided the experimental results for this specific failure are available and the corresponding reference driving force controlling such a failure is recognized. The reference driving force is characterized by the different Weibull distribution obtained, which influences the resulting predictions for brittle and ductile type of failure.
The authors [3] draw attention to the need to apply the statistical technique denoted confounded data [8,9]. This approach allows the cumulative distribution functions (CDF) for any of the flaw populations to be separately achieved without neglecting the mutual statistical interference between several distributions. In the present study, an extension of such a probabilistic failure approach is presented allowing the consideration of different constitutive equation of the material behavior, as well as the influence of scale effects, when specimens of different size are tested. The results are compared for states when the most suitable failure generalized parameter to determine the probability of failure is identified among three alternatives, namely, elastic solution, classical J_2 theory of plasticity and strain gradient plasticity theory.

PROBABILISTIC MODEL

The model for a probability–statistical assessment used in this study is based on a generalized local model, described in [3–7]. This generalized probabilistic local approach (GPLA) allows a direct relationship to be found between the critical reference variable, as defined by the fracture criterion, and the failure probability. The relationship, known as primary failure cumulative distribution function (PFCDF) can be expressed by means of a three parameter Weibull cumulative distribution function (CDF) [10]. Accordingly, the failure probability P_{fail} of an element subjected to a certain critical factor X_c uniformly distributed on the element can be represented as follows

$$P_{fail} = 1 - \exp\left[-\left(\frac{GP - \lambda}{\delta} \right)^{\beta} \right] \tag{1}$$

where λ, β and δ are, respectively, the location parameter, the shape parameter and the scale parameter associated with the selected reference area. Generalized parameter GP in Eq.1 is determined in terms of the driving force for accepted either brittle or ductile failure criterion.
The following is the iterative procedure applied to achieve fitting of the optimal primary distribution function from an experimental data set exhibiting three different failure types. It implies estimation of the nine Weibull parameters, three for any of the failure mechanisms. Fig. 1 shows a flaw chart that describes the iterative procedure applied consisting in the following steps:

- In an experimental program, failure tests are carried out and the corresponding results for the critical parameter determined.
- The loading process up to failure for any test is simulated by means of a finite element code. In this way, the type and value of the driving force at failure for any element are known.
- The failure results are ranked in increasing order according to the value of the driving force reached by any specimen at failure. Subsequently, using Bernard's expression [11]:

$$P_{fail,i} = \frac{i - 0.3}{N + 0.4} \tag{2}$$

the accumulated failure probability is provided for any population individually referred to the specific specimen size and failure type obtained. In Eq.2 $i = 1, ..., N$, and N is the number of cases studied.

- The Weibull parameter are estimated by applying Eq.1 to the generalized parameter and the failure probability as obtained for any test. Once fitting is accomplished, the value of the nine Weibull parameters are estimated for the iteration being.
- With the aim of assessing the convergence of the procedure, the parameter values obtained at any iteration are compared with those found in the preceding iteration until the summation of the variations in the values of each of them is less than a prescribed threshold value ε:

$$\left|\lambda_i-\lambda_{i-1}\right|+\left|\beta_i-\beta_{i-1}\right|+\left|\delta_i-\delta_{i-1}\right|<\varepsilon \tag{3}$$

When this occurs, the parameter values obtained in the last iteration are considered to be the final solution.

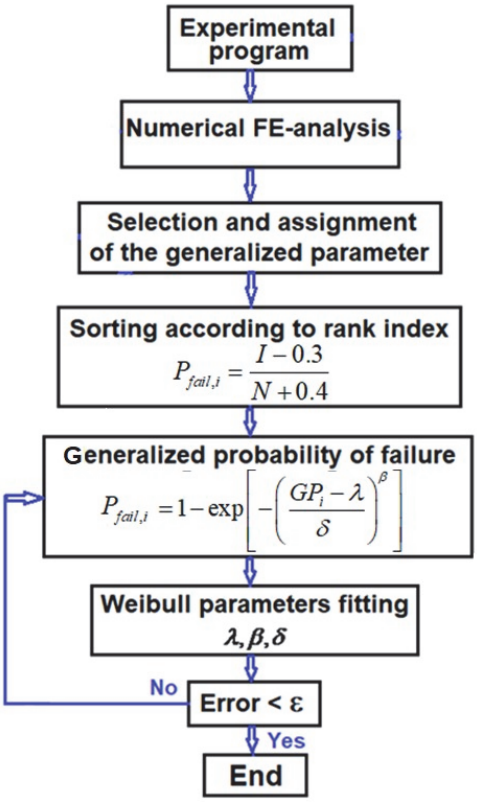

Figure 1: Flow-chart representing the iterative procedure applied for data fitting.

As can be observed, the procedure proposed is implemented by merely mentioning without specifying the "failure criterion" bound to the driving force being considered. This allows the approach to be applicable to any specific failure problem handled irrespective of its complexity provided the weakest link principle is applicable referred to either brittle or ductile failure.

GENERALIZED PARAMETERS

In this section we will consider both elastic and nonlinear formulations for the generalized parameter which characterizes the fractures of the tested specimens according to brittle and ductile failure criteria. Three GPs were analyzed in this study, related to the following fracture parameters: elastic stress intensity factor (SIF) K_I (GP_{KI}), plastic stress intensity factor K_p (GP_{Kp}) based on the classical J_2 Hutchinson-Rice-Rosengren (HRR) solution, and plastic SIF K_{SGP} (GP_{Ksgp}) backgrounded on strain gradient plasticity theory.

ELASTIC GENERALIZED PARAMETER GPK1

The values of the elastic SIF K_I were obtained in accordance with standard ASTM E399 [12] by the following equations. For the compact tension C(T) configuration:

$$K_1 = \frac{P_q}{B\sqrt{W}} Y_1\left(\frac{a}{W}\right)$$

$$Y_1\left(\frac{a}{W}\right) = \frac{\left(2+a/W\right)}{\left(1-a/W\right)^{1.5}}\left(0.886+4.64\left(\frac{a}{W}\right)-13.31\left(\frac{a}{W}\right)^2+14.72\left(\frac{a}{W}\right)^3-5.6\left(\frac{a}{W}\right)^4\right) \tag{4}$$

and for the single-edge-notched bend (SENB) configuration:

$$K_1 = \frac{P_q L_1}{BW^{3/2}} Y_1\left(\frac{a}{W}\right)$$

$$Y_1\left(\frac{a}{W}\right) = 1.93-3.07\left(\frac{a}{W}\right)+14.53\left(\frac{a}{W}\right)^2-25.11\left(\frac{a}{W}\right)^3+25.8\left(\frac{a}{W}\right)^4 \tag{5}$$

where a is the crack length, B is the specimen thickness, W is the specimen width, L_1 is the span of the bending specimen, and Y_1 is the geometry-dependent SIF correction factor. The values of the P_Q loads were obtained using the typical load versus load-line crack opening displacement curves for the C(T) and SENB configurations.

HRR-PLASTIC GENERALIZED PARAMETER GP_{KP}

The classical HRR singular solution [13,14] for an infinite size cracked body of a strain-hardening material was completed by Shlyannikov and Tumanov as numerical method [15] for plastic stress intensity factor determination applied to mixed mode plane strain/plane stress problems and general three-dimensional (3D) structural element configurations. According to this method, the plastic SIF K_p can be expressed directly in terms of the corresponding elastic SIF K_I:

$$\bar{K}_P = \left[\left(\frac{\sigma_{yn}}{\sigma_0}\right)^2 \frac{\pi\left(\bar{K}_1^2\right)}{\alpha I_n}\left(\frac{a}{W}\right)\right]^{1/(n+1)} \tag{6}$$

where a and n are the strain hardening parameters, σ_{yn} is the nominal stress, σ_0 is the yield stress, and I_n is the governing parameter of the elastic–plastic stress–strain fields in the form of dimensionless factor:

$$I_n^{FEM}\left(\theta,n,\left(a/w\right)\right) = \int_{-\pi}^{\pi} \Omega^{FEM}\left(\theta,n,\left(a/w\right)\right) d\theta$$

$$\Omega^{FEM}\left(\theta,n,\left(a/w\right)\right) = \frac{n}{n+1}\left(\tilde{\sigma}_e^{n+1}\right)^{FEM}\cos\theta - \left[\tilde{\sigma}_{rr}^{FEM}\left(\tilde{u}_\theta^{FEM} - \frac{d\tilde{u}_r^{FEM}}{d\theta}\right) - \tilde{\sigma}_{r\theta}^{FEM}\left(\tilde{u}_r^{FEM} + \frac{d\tilde{u}_\theta^{FEM}}{d\theta}\right)\right]\sin\theta - \tag{7}$$

$$-\frac{1}{n+1}\left(\tilde{\sigma}_{rr}^{FEM}\tilde{u}_r^{FEM} + \tilde{\sigma}_{r\theta}^{FEM}\tilde{u}_\theta^{FEM}\right)\cos\theta$$

In this case, the numerical integral of the crack-tip field I_n changes not only with the strain-hardening exponent n, but also with the relative crack length a/W and specimen configuration. Numerical results regarding the behavior of the I_n-integral in the most common experimental configurations for test specimens in fracture mechanics can be found in Refs. [16–18].

SGP-PLASTIC GENERALIZED PARAMETER GPKSGP

The third generalized parameter is presented in the form of a plastic stress intensity factor based on the strain gradient plasticity (SGP) theory. In this case the aim of the conventional mechanism-based strain gradient plasticity theory [19-21] is to capture the role of geometrically necessary dislocation (GND) density in the mechanics of crack initiation and growth. The advantage of SGP plasticity theory, which grounded on the Taylor's dislocation model [22], is sensitivity to the intrinsic material plastic length parameter ℓ. According to SGP theory, the tensile flow stress is related to a reference stress σ_{ref}, the equivalent plastic strain ε_p and the effective plastic strain gradient η^p:

$$\sigma_{flow} = \sigma_{ref}\sqrt{f^2\left(\varepsilon^P\right) + l\eta^P} \tag{8}$$

where

$$l = 18\alpha^2\left(\mu/\sigma_{ref}\right)^2 b \tag{9}$$

Here, $\bar{a}$ is an empirical coefficient that is assumed to be equal to 0.5, μ is the shear modulus and b is the Burgers vector length. The first-order version of the conventional mechanism-based strain gradient (CMSG) plasticity model is implemented in the computation of the material Jacobian and, consequently, of the rate of the stress tensor:

$$\dot{\sigma}_{ij} = K\dot{\varepsilon}_{kk}\delta_{ij} + 2\mu\left[\dot{\varepsilon}'_{ij} - \frac{3\dot{\varepsilon}}{2\sigma_e}\left(\frac{\sigma_e}{\sigma_{flow}}\right)^m \sigma'_{ij}\right] \tag{10}$$

where $\dot{\varepsilon}'_{ij}$ is the deviatoric strain rate tensor. As with other continuum strain gradient plasticity models, the CMSG theory is intended to model a collective behaviour of dislocations and is therefore not applicable at scales smaller than the dislocation spacing.

Taking into account the singular nature of the stress distribution at the crack tip for the CMSG plasticity theory of plasticity Eqs.8-10, Shlyannikov et al. [23-25] introduced a new plastic stress intensity factor in the following form:

$$\bar{\sigma}_e^{FEM}\left(r,\theta\right) = K_{SGP}^{FEM}\,\bar{r}^{\gamma}\,\hat{\sigma}_e^{FEM}\left(r,\theta\right) \tag{11}$$

$$A_P^{FEM}\left(r,\theta\right) = \bar{\sigma}_{ij}^{FEM}\left(r,\theta\right)\Big/\hat{\sigma}_{ij}^{FEM}\left(r,\theta\right) \tag{12}$$

$$K_{SGP}^{FEM} = A_P^{FEM}\Big/\bar{r}^{\gamma} \tag{13}$$

where $\bar{r} = r/l$ is the normalized distance to the crack tip, and γ is the power of the stress singularity. In Eq.11, the angular distributions of the dimensionless stress component $\hat{\sigma}_{ij}^{FEM}\left(r,\theta\right)$ are normalized, such that $\hat{\sigma}_{e,\max}^{FEM} = \left(3/2\,S_{ij}^{FEM}S_{ij}^{FEM}\right)_{\max}^{1/2} = 1$ and $\bar{\sigma}_{ij}^{FEM} = \sigma_{ij}^{FEM}\Big/\sigma_Y$. In the further presentation of numerical and experimental results, we will use the following notation for plastic SIF $K_{SGP}^{FEM} = K_{SGP}$.

In this study, tested compact and bending specimens made of 34XH3MA and S55C steels are considered as a subject for application of the conventional elasticity, the classical J2 and CMSG plasticity theories. The implementation of a mechanism-

based SGP theory in ANSYS [26] using a user material subroutine USERMAT has been described in more detail by the authors [23-25].

MATERIAL PROPERTIES AND NUMERICAL DATA

The algorithm described in Section 2 was used for the probabilistic assessment based on the experimental data. Several experiments and corresponding numerical calculations were performed on CT and SENB specimen configurations produced from steels 34XH3MA and JS55C. The fracture toughness tests were performed in accordance with ASTM E399 [12]. The experimental data for the fracture toughness characteristics of the SENB specimens of JS55C steel were obtained from Meshii et al. [27].

The main mechanical properties of the analyzed materials are listed in Tab. 1, where E is the Young's modulus, σ_0 is the yield stress, σ_f is the tensile strength, σ_u is the true ultimate tensile stress, a is the strain hardening coefficient, and n is the strain hardening exponent.

Steel	E, GPa	σ_0, MPa	σ_f, MPa	σ_u, MPa	a	n
34XH3MA	216.2	714.4	1040	1260	0.529	7.89
JS55C	212.4	393	703	1274	1.265	5.45

Table 1: Main mechanical properties of the steels.

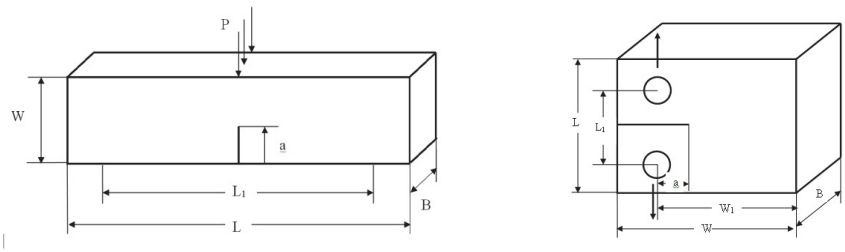

a) b)

Figure 2: SENB (a) and C(T) (b) specimen configuration.

The loading configuration and specimen geometry are shown in Fig. 2. The relative crack length a/W and relative thickness B/W were varied for each specimen configuration. The relative crack length a/W was varied in the range of 0.245–0.645. Three types of C(T) specimens with B/W ratios of 0.125, 0.25, and 0.5 and four types of SENB specimens with B/W ratios of 0.25, 0.5, 1.0, and 1.5 were used. The specimen sizes and crack lengths are listed in Tab. 2.

A full-field 3D finite-element analysis was performed using the experimental set of P_q loads for each tested specimen to determine the elastic–plastic stress fields along the through-thickness crack front in the SENB and C(T) specimens subjected to bending and tension loadings. In all numerical calculations for a strain-hardening material with a pure power-law behavior, the Ramberg–Osgood constitutive relationship with n, a, and σ_0 constants, listed in Tab. 1, was used. The numerical calculations for the conventional mechanism-based strain gradient plasticity model according to the constitutive Eqs.8-10 were performed for the value of the intrinsic material plastic length parameter ℓ = 5 μm.

To accurately characterize the strain gradient effect, a high-density FE mesh was formed near the crack tip and along crack front in SENB and C(T) specimens. The FE-mesh sensitivity parametric study shown that a quadrilateral brick element size less than 0.15 μm provided mesh-independent results. For the elastic-plastic analysis of both specimen FE models, the initial crack tip was assigned a radius of curvature ϱ = 0.87 μm. A typical FE mesh for the C(T) specimen configuration has 9,625,812 nodes, while for the SENB specimen has 17,903,812 nodes. The ANSYS [26] finite-element code was applied to obtain the distribution of stresses along the crack front for the tested specimen, which were used to determine both the elastic and nonlinear stress intensity factors. The obtained GPs in the form of elastic and plastic SIFs for all specimen configurations are listed in Tab. 2.

RESULTS AND DISCUSSION

In this work, the method of confounded data is employed to the consideration of the cumulative distribution functions (cdf) for three flaw populations, characterized by corresponding the generalized parameters, namely, elastic K_I and two types of plastic K_P and K_{SGP} stress intensity factors. The first of them represent brittle material behavior, while the second and third parameters are related to ductile fracture. The maximum elastic or plastic stress intensity factor is considered to be the critical parameter (GP) under static failure conditions. Recall that, the method of confounded data allows the cumulative distribution functions for any of the flaw populations to be separately achieved.

Material	Specimen type	W, mm	B, mm	B/W	a/W	a, mm	K_1	K_P	K_{SGP}
34XH3MA	C(T)	40	20	0.5	0.350	14.0	66.012	0.6965	1.301
					0.350	14.0	63.343	0.6864	1.308
					0.625	25.0	62.72	0.6860	1.302
					0.645	25.8	68.152	0.6965	1.342
			10	0.25	0.380	15.2	77.563	0.7209	1.401
					0.425	17.0	78.99	0.7245	1.441
					0.475	19.0	77.551	0.7188	1.490
					0.487	19.5	76.35	0.7140	1.399
			5	0.125	0.380	15.2	71.4	0.7071	1.332
					0.358	15.4	60.67	0.682	1.269
					0.4625	18.5	70.17	0.7021	1.330
					0.475	19.0	69.44	0.6995	1.326
34XH3MA	SENB	20	10	0.5	0.245	4.9	68.12	0.7945	1.288
					0.250	5.0	57.24	0.7629	1.272
					0.445	8.9	64.35	0.7659	1.289
					0.445	8.9	57.5	0.7576	1.310
					0.610	12.2	55.25	0.745	1.285
					0.615	12.3	57.53	0.7525	1.238
			20	1	0.605	12.1	52.146	0.7289	1.232
					0.620	12.4	55.964	0.7328	1.258
S55C	SENB	25	6.25	0.25	0.507	12.67	58.112	0.709	1.985
					0.501	12.53	67.492	0.75	2.442
					0.499	12.47	58.12	0.7	1.872
					0.503	12.58	65.81	0.732	2.232
					0.500	12.51	67.79	0.744	2.323
			12.5	0.5	0.500	12.49	55.214	0.699	1.891
					0.504	12.61	63.259	0.733	2.329
					0.5008	12.52	56.896	0.71	1.983
					0.5028	12.57	61.94	0.725	2.120
					0.5016	12.54	61.359	0.722	2.104
			25.0	1.0	0.497	12.43	59.295	0.722	1.943
					0.498	12.45	59.24	0.715	1.935
					0.502	12.54	62.902	0.741	2.149
					0.497	12.43	62.17	0.735	2.064
			37.5	1.5	0.494	12.35	60.122	0.723	1.897
					0.502	12.56	62.74	0.733	2.031
					0.499	12.48	64.635	0.749	2.132
					0.501	12.53	61.516	0.73	2.039

Table 2: Generalized parameters for tested specimens.

PRIMARY FAILURE CUMULATIVE DISTRIBUTION FUNCTION

In order to illustrate the methodology applied for checking the suitability of the failure criterion, as represented by an adequate generalized parameter (GP), taking into account the critical parameter distribution and the size of the specimen tested the following examples are exposed. Three experimental programs consisting of SENB and C(T) specimen tests with different sizes (Tab. 2) are simulated. For each of the considered generalized parameter, we distinguish three separate populations: SENB specimen from JS55C steel, SENB specimen from 34XH3MA steel and C(T) specimen from 34XH3MA steel. Thus, we will consider the behavior of two different materials that are implemented on test samples of two configurations.

	K_1			K_P			K_{SGP}		
	JS55C SENB	34XH3M SENB	34XH3M C(T)	JS55C SENB	34XH3M SENB	34XH3M C(T)	JS55C SENB	34XH3M SENB	34XH3M C(T)
λ	55.697	51.103	57.030	0.643	0.707	0.668	1.835	1.220	1.256
δ	7.782	8.395	15.019	0.089	0.054	0.039	0.277	0.060	0.109
β	1.456	1.359	1.986	6.079	2.459	2.477	1.481	1.595	1.479

Table 3: The resulting three-parameter Weibull distribution characteristics for tested steels.

Test data are simulated assuming that N=18 SENB specimens from JS55C, N=8 SENB specimens from 34XH3MA and N=12 C(T) specimens from 34XH3MA are loaded up to failure, which may caused by three different initiating failure mechanisms related to elasticity, classical and strain gradient plasticity. In this experimental program, the values of the failure load for each test is registered from which the corresponding driving force (in this case, stress intensity factors) distribution at failure is determined using a finite element code. Thereafter, the FEM results are used for estimating the three sets of Weibull parameters corresponding to any failure type following the steps as indicated above. Making use of the data numerically simulated, nine cdfs are fitted separately. The Weibull parameters being found in this procedure are listed in Tab. 3, from which the adequacy of the fitting performed is apparent, provided a sufficient number of experimental data results are at disposal.

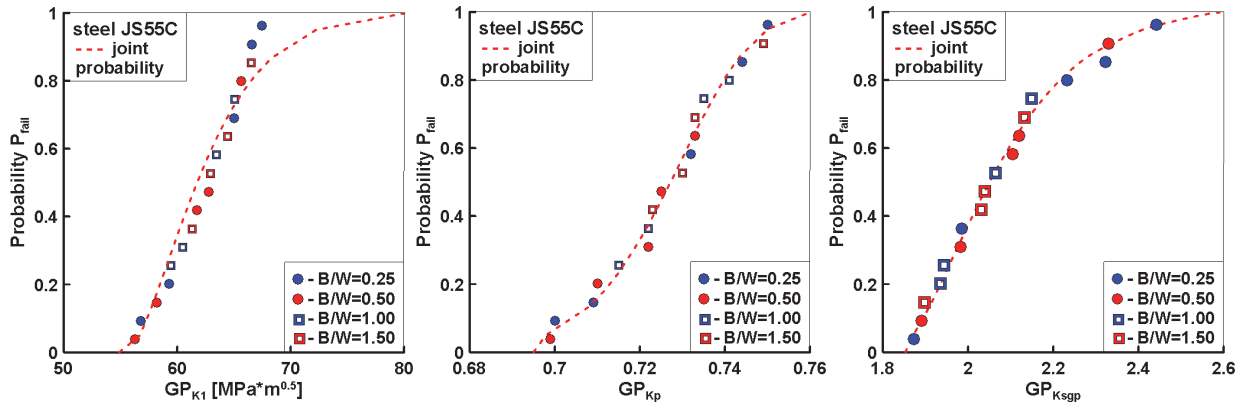

Figure 3: Probabilities of failure for (a) elastic, (b) plastic K_P and (c) K_{SGP} SIFs for SENB JS55C steel specimens.

Figs. 3-5 represent the experimental failure cumulative distribution function (EFCDF) for each test type and their fitting by Eq.1. As shown in Figs. 3-5, the PFCDF leads to a satisfactory adjustment of the experimental results for each experimental programs have been implemented on SENB and C(T) test samples produced from JS55C and 34XH3MA steels, which would not be possible if the failure criterion were unsuitable. However, as can be observed, the primary failure cumulative distribution function, based on the nonlinear generalized parameters (plastic SIFs K_P and K_{SGP}), give more uniform behavior with respect to the GP related with elastic SIF K_I. The use of the material property PFCDF (Figs. 3-5) in combination with the Weibull parameters (Tab. 3) generated for each experiment permits us to conclude that the division into three external (K_I, K_P and K_{SGP}) and three internal (SENB-JS55C, SENB-34XH3MA and C(T)-34XH3MA) populations was justified.

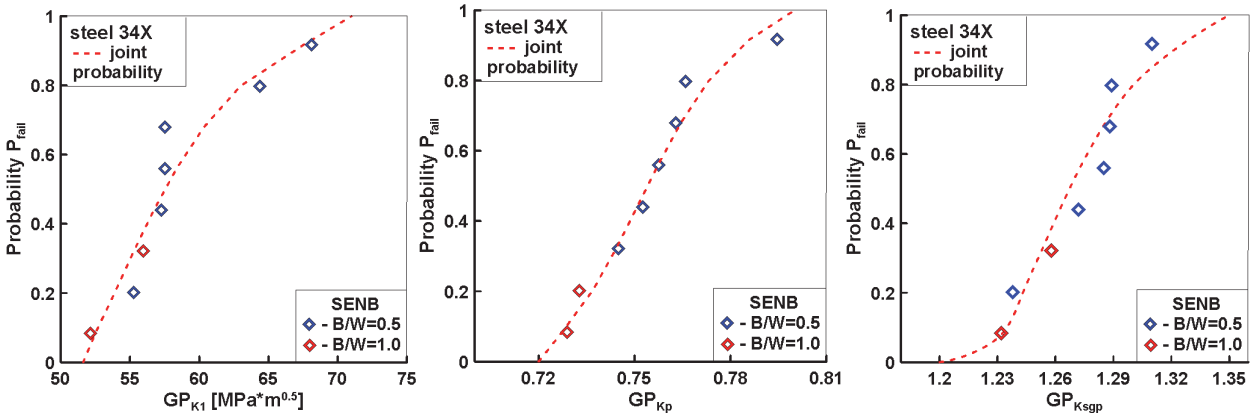

a) b) c)

Figure 4: Probabilities of failure for (a) elastic, (b) plastic K_P and (c) K_{SGP} SIFs for SENB 34XH3MA steel specimens.

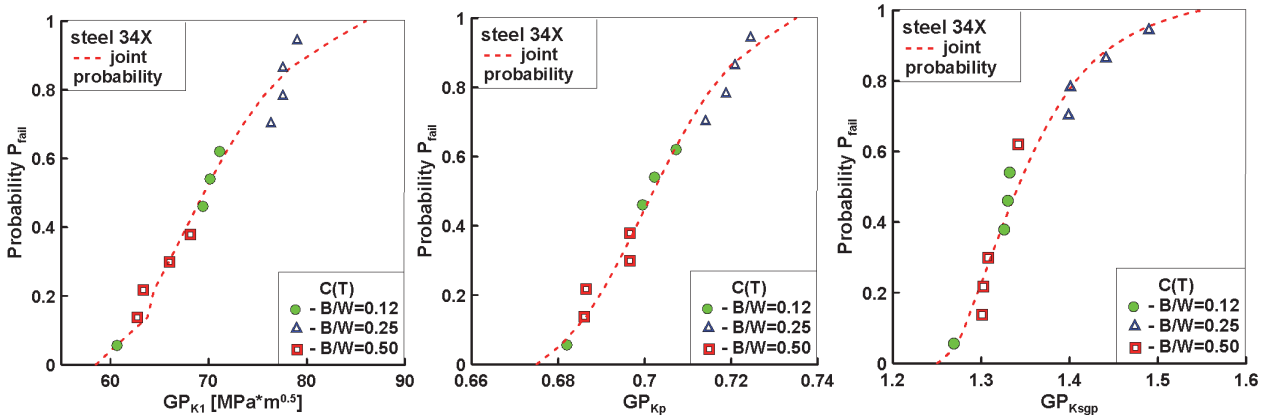

a) b) c)

Figure 5: Probabilities of failure for (a) elastic, (b) plastic K_P and (c) K_{SGP} SIFs for C(T) 34XH3MA steel specimens.

Figs. 3-5 show probability diagrams as a function of the elastic SIF K_I, plastic SIFs K_P and K_{SGP} for JS55C and 34XH3MA steels with different ranges of values and scales, which make it not convenient to compare the PFCDF in specimens with different thicknesses and configurations. Using only the information as presented so far is impossible to determine if a test specimen subjected to bending or tension loading, characterized by elastic generalized parameter, has higher or lower probability of failure than the same sample interpreted in terms of plastic GPs. In addition, it is not clear whether there are differences in the assessments of the failure probability from the point of view of the classical and modern gradient theories of plasticity.

DIMENSIONLESS GENERALIZED PARAMETERS

To overcome these problems, the authors proposed for representing the results the following normalized coordinates for each of the generalized parameters:

$$GP_n = \frac{GP_i - GP_{\min}}{GP_{\max} - GP_{\min}} \tag{14}$$

where GP_{min} and GP_{max} are the minimum and maximum values of the GP for each failure probability diagram, respectively; GP_i denotes the current value of the generalized parameter; $n = K_I, K_P, K_{SGP}$. In the following analysis of the experimental results, we use the PFCDF and the dimensionless variables GP_n which change in the range from 0 to 1. The dimensionless

GP_n enables the arrangement of the generalized parameters depending on the probability of failure and identification of the GP having the largest probability of failure at a given material and the specimen configuration.
Fig. 6 summarizes the failure probability P_{fail} versus the dimensionless GP_n in terms of elastic K_I and plastic K_P, K_{SGP} SIFs for JS55C (Fig. 6a) and 34XH3MA (Figs. 6b, c) steels based on Eq.14. As can be seen, the primary failure cumulative distribution function, related to the elastic and nonlinear generalized parameters do not match each other for the three internal populations (SENB-JS55C, SENB-34XH3MA and C(T)-34XH3MA). This conclusion once again confirms the possibility of applying the statistical technique known as confounded data to the analysis of elastic-plastic problems of fracture mechanics. Since the reference driving force is different (elastic K_I and plastic K_P and K_{SGP} SIFs), the type of failure is characterized by the different Weibull distribution obtained, which influences the resulting predictions for either brittle or ductile type of fracture.

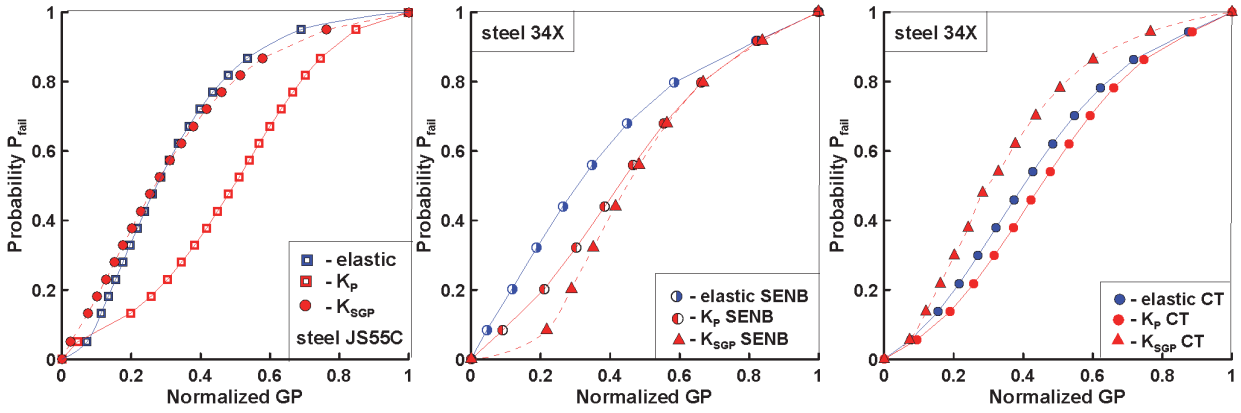

a) b) c)

Figure 6: Probabilities of failure versus normalized GP for (a) and (b) SENB and (c) C(T) specimens in terms of elastic and plastic SIFs.

In Fig. 6a, for SENB sample made of JS55C steel, the elastic solution (GP_{KI}) and the theory of gradient plasticity (GP_{Ksgp}) predict approximately the same probability of failure, while the classical theory of plasticity (GP_{Kp}) gives significantly underestimated results. In SENB specimen made of 34XH3MA steel, the elastic solution shows the highest probability of failure (Fig. 6b), and the nonlinear solutions are close to each other. In a compact C(T) sample of that material, the highest probability of failure corresponds to strain gradient plasticity theory (Fig. 6c). Summarizing the presented results, we can say that the observed differences in the probability of failure are due to the use of various constitutive equations of material behavior in the range from elasticity to gradient plasticity.
The failure cumulative distribution functions P_{fail} and normalized GPs may be interpreted as material characteristics enabling the prediction of the failures of structure elements depending on the formulation of the constitutive equation of the material behavior. The failure distribution functions of the SENB and compact C(T) specimens of 34XH3MA steel were compared in Figs. 7a, b to analyze the influences of the sample configuration with the elastic and plastic approaches of fracture mechanics point of view. As observed in these figures, the probabilities of failure based on the elastic solution (Fig. 7a, GP_{KI}) and plastic solution (Fig. 7b, GP_{Kp} and GP_{Ksgp}) for the two test specimen geometries do not coincide with each other. Differences in the distributions of the failure probability increase in the transition from elastic to plastic analysis. Moreover, a higher failure probability is predicted by the gradient theory of plasticity when applied to a compact sample.
For the same geometry of the bending sample, Figs.7c, d represent the results of assessing the influence of the elastic-plastic properties of the steels under consideration. Recall that JS55C and 34XH3MA steels (Tab. 1) have approximately the same elastic properties (E and Poisson's ratio ν), but differ significantly in plastic (σ_0, a, n) and fracture resistance (σ_f, σ_u) characteristics. The failure probability distribution functions of the same SENB specimen configuration for elastic solution in terms of GP_{KI} are shown in Fig. 7c for the considered materials. As expected for the elastic conditions, the distribution curves are considerably close to each other with a slight difference at high values of the failure probability. Fig. 7d shows a comparison of results for SENB specimen of JS55C and 34XH3MA steels for two plasticity theories based on the classical approach (GP_{Kp}) and plastic strain gradient effects (GP_{Ksgp}). As can be seen, significant differences in these nonlinear solutions take place in the more ductile steel JS55C. In this case, a high fracture probability corresponds to the generalized parameter for gradient plasticity. Obviously, this is due to the fact that in the gradient plasticity theory, in comparison with the classical J_2 theory, an additional parameter in the form of the intrinsic material plastic length scale ℓ is added to the set of traditional material properties (E, ν, σ_0, a, n).

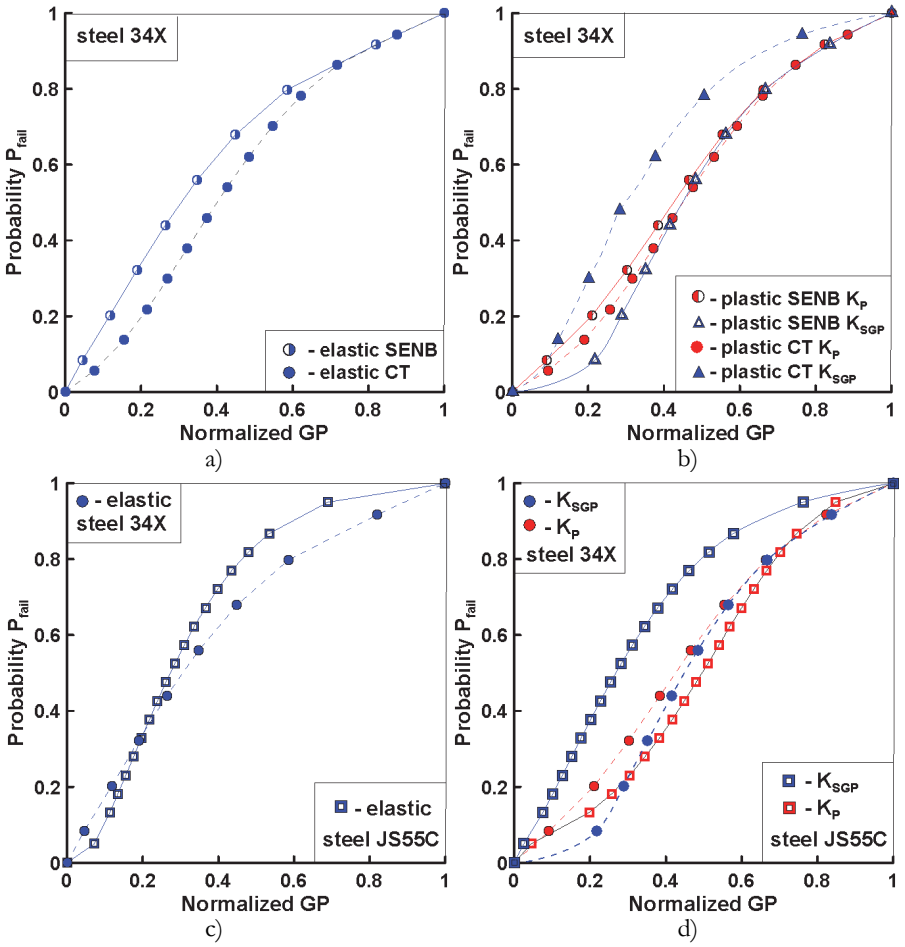

Figure 7: Comparison of failure probability versus normalized GP for elastic and nonlinear solutions, (a) and (b) 34XH3MA steel, (c) and (d) JS55C and 34XH3MA steels.

CONCLUSIONS

The principal conclusions of the present study are:

- The application of the confounded data concept allows the primary failure cumulative distribution functions to be obtained for elastic and ductile fracture types that may appear in an experimental test campaign.
- The comparison of the results obtained from the experimental programs carried out on SENB and C(T) specimens of different sizes from JS55C and 34XH3MA steels is possible using the Weibull parameters estimated from the elastic and plastic generalized parameter behaviors.
- The applicability and suitability proposed of the normalized generalized parameters are confirmed by means of an example using simulated data corresponding to elastic and nonlinear fracture mechanics approaches.
- It is assumed that the use of nonlinear generalized parameters in comparison with elastic ones is justified due to the fact that in some cases the gradient theory of plasticity predicts the highest probability of failure.

ACKNOWLEDGEMENTS

The authors gratefully acknowledge the financial support of the Russian Science Foundation under the Project 20-19-00158.

REFERENCES

[1] Wentzel, E.S. (1969). Probability Theory, Science, Moscow.

[2] Weibull, W. (1951). A statistical distribution function of wide applicability, J. Appl. Mech., 18(3), pp. 293-297.

[3] Muñiz-Calvente, M., Fernández Canteli, A., Shlyannikov, V., Castill, E. (2015). Probabilistic Weibull methodology for fracture prediction of brittle and ductile materials, Appl. Mech. Mater., 784, pp. 443-451. DOI: 10.4028/www.scientific.net/AMM.784.443.

[4] Muñiz-Calvente, M., Fernández-Canteli, A. (2016). Joint evaluation of fracture and fatigue results from distinct specimen size and geometry, Proced. Struct. Integr., 1, pp. 142-149. DOI: 10.1016/j.prostr.2016.02.020.

[5] Muñiz-Calvente, M., Shlyannikov, V., Meshii, T., Giner, E., Fernández-Canteli, A. (2016). Joint evaluation of fracture results from distinct test conditions, implying loading, specimen size and geometry, Proced. Struct. Integr., 2, pp. 720-727. DOI: 10.1016/j.prostr.2016.06.093.

[6] Muñiz-Calvente, M., Ramos, A., Pelayo, F., Lamela, M., Fernández-Canteli, A. (2016). Statistical joint evaluation of fracture results from distinct experimental programs: An application to annealed glass, Theoret. Appl. Fract. Mech., 85 (Part A), pp. 149-157. DOI: 10.1016/j.tafmec.2016.08.009.

[7] Vantadori, S., Muñiz-Calvente, M., Scorza, D., Fernández-Canteli, A., Álvarez Vázquez, A., Carpinteri, A. (2018). The generalised local model applied to fibreglass, Compos. Struct., 202, pp. 1353-1360. DOI: 10.1016/j.compstruct.2018.06.073.

[8] Castillo, E., Fernández-Canteli, A., García-Prieto, M.A., Lamela, M.J. (2004). Strength characterization of glass by means of the statistical theory of confounded data, Key Eng. Mater., 264-268, pp. 1923-1926. DOI: 10.4028/www.scientific.net/KEM.264-268.1923.

[9] Przybilla, C., Fernández-Canteli, A., Castillo, E. (2013). Maximum likelihood estimation for the three-parameter Weibull cdf of strength in presence of concurrent flaw populations, J. Eur. Ceram. Soc., 33, pp. 1721-1727.

[10] Muñiz-Calvente, M., Ramos, A., Shlyannikov, V., Lamela, M., Fernández-Canteli, A. (2016). Hazard maps and global probability as a way to transfer standard fracture results to reliable design of real components, Eng. Fail. Anal., 69, pp. 135-146. DOI: 10.1016/j.engfailanal.2016.02.004.

[11] Bernard, A., Bos-Levenbach, E. (1955). The plotting of observations on probability-paper, Stichting Mathematisch Centrum. Statistische Afdeling.

[12] ASTM E399-90 (1997). Standard test method for plane-strain fracture toughness of metallic materials. Annual book of ASTM standards. Philadelphia (PA): American Society for Testing and Materials. DOI: 10.1520/E0399-90R97.

[13] Hutchinson, J.W. (1968). Singular behaviour at the end of a tensile crack in a hardening material, J. Mech. Phys. Solids, 16 (1), pp. 13-31. DOI: 10.1016/0022-5096(68)90014-8.

[14] Rice, J.R., Rosengren, G.F. (1968). Plane strain deformation near a crack tip in a power-law hardening material, J. Mech. Phys. Solids, 16 (1), pp. 1-12. DOI: 10.1016/0022-5096(68)90013-6.

[15] Shlyannikov, V., Tumanov, A. (2014). Characterization of crack tip stress fields in test specimens using mode mixity parameters, Int. J. Fract., 185, pp. 49-76. DOI: 10.1007/s10704-013-9898-0.

[16] Shlyannikov, V.N., Boychenko, N.V., Tumanov, A.V., Fernández-Canteli, A. (2014). The elastic and plastic constraint parameters for three-dimensional problems, Eng. Fract. Mech., 127, pp. 83-96. DOI: 10.1016/j.engfracmech.2014.05.015.

[17] Shlyannikov, V.N. (2013). T-stress for crack paths in test specimens subject to mixed mode loading, Eng. Fract. Mech., 108, pp. 3-18. DOI: 10.1016/j.engfracmech.2013.03.011.

[18] Shlyannikov, V.N., Zakharov, A.P. (2014). Multiaxial crack growth rate under variable T-stress, Eng. Fract. Mech., 123, pp. 86-99. DOI: 10.1016/j.engfracmech.2014.02.013.

[19] Gao, H., Huang, Y., Nix, W.D., Hutchinson, J.W. (1999). Mechanism-based strain gradient plasticity—I. Theory, J. Mech. Phys. Solids, 47 (6), pp. 1239-1263. DOI: 10.1016/S0022-5096(98)00103-3.

[20] Qiu, X., Huang, Y., Wei, Y., Gao, H., Hwang, K.C. (2003). The flow theory of mechanism-based strain gradient plasticity, Mech. Mater., 35 (3-6), pp. 245-258. DOI: 10.1016/S0167-6636(02)00274-0.

[21] Huang, Y., Qu, S., Hwang, K.C., Li, M., Gao, H. (2004). A conventional theory of mechanism-based strain gradient plasticity, Int. J. Plast., 20 (4-5), pp. 753–782. DOI: 10.1016/j.ijplas.2003.08.002.

[22] Taylor, G.I. (1938). Plastic strain in metals, J. Inst. Metals, 62, pp. 307–324.

[23] Shlyannikov, V., Martínez-Pañeda, E., Tumanov, A., Tartygasheva, A. (2021). Crack tip fields and fracture resistance parameters based on strain gradient plasticity, Int. J. Solids Struct., 208-209, pp. 63-82. DOI: 10.1016/j.ijsolstr.2020.10.015.

[24] Shlyannikov, V., Martínez-Pañeda, E., Tumanov, A., Khamidullin, R. (2021). Mode I and mode II stress intensity factors and dislocation density behaviour in strain gradient plasticity, Theoret. Appl. Fract. Mech., 116, 103128. DOI: 10.1016/j.tafmec.2021.103128.
[25] Fedotova, D., Khamidullin, R., Shlyannikov, V. (2022). Inversion of dislocation densities under mixed mode fracture, Eng. Fail. Anal., 138, 106311. DOI: 10.1016/j.engfailanal.2022.106311.
[26] ANSYS Mechanical APDL Theory Reference Release 21.R1. (2021). ANSYS, Inc. Southpointe, 275 Technology Drive, CanonBurg, PA.
[27] Meshii, T., Lu, K., Takamura, R. (2013). A failure criterion to explain the test specimen thickness effect on fracture toughness in the transition temperature region, Eng. Fract. Mech., 104, pp. 184-197. DOI: 10.1016/j.engfracmech.2013.03.025.